

PACS 33.20.Fb; 36.40.Gk; 73.20.Mf; 78.30.-j

SERS of Rhodamine 6G on substrates with laterally ordered and random gold nanoislands

**V.O. Yukhymchuk¹, S.A. Kostyukevych¹, V.M. Dzhagan¹, A.G. Milekhin²,
E.E. Rodyakina², I.B. Yanchuk¹, P.Ye. Shepeliavy¹, M.Ya. Valakh¹,
K.V. Kostyukevych¹, V.O. Lysiuk¹, I.V. Tverdokhlib³**

¹*V. Lashkaryov Institute of Semiconductor Physics, NAS of Ukraine, pr. Nauky 45, Kyiv 03028, Ukraine*

²*A.V. Rzhanov Institute of Semiconductor Physics, pr. Lavrentieva, 13, Novosibirsk 630090, Russia*

³*Specialized Enterprise "Holography" Ltd., 64 Lenin str., Kyiv 02088, Ukraine*

E-mail: yukhym@isp.kiev.ua

Abstract. Preparation and study of laterally ordered and disordered arrays of Au nanoislands as SERS substrates are reported. Developed technology allows obtaining SERS substrates with long-term stability (up to six months), efficient (up to 10^4) and laterally homogenous enhancement of the Raman signal from molecular analyte. The substrates developed are suitable for Raman bio-diagnostics, because their plasmon resonance can be tuned within the range 700-900 nm that falls into the transparency window of human tissues. The dependence of optical and enhancement properties of the substrates on their morphology has been studied. The morphology of the Au island film and their plasmon resonance spectrum depend noticeably on the nominal Au thickness and post-annealing temperature, while the duration of annealing is of minor importance. Formation of nanoholes in the case of Au substrates on holographically pre-patterned polymer film opens up the possibility of additional Raman enhancement via the "hot spot"-effect.

Keywords: SERS substrates, plasmon, gold nanoislands, Rhodamine 6G.

Manuscript received 08.05.12; revised version received 25.05.12; accepted for publication 14.06.12; published online 25.09.12.

1. Introduction

Optical properties of micro- and nanosized metal nanoparticles obtained by various physical and chemical methods have been intensively investigated both experimentally and theoretically in the recent years [1-9]. The huge interest to this kind of nanostructures is caused by interesting fundamental effects in metals of decreased dimensionality and by their promising applications. In particular, the availability of tunable plasmon resonances in metal nanostructures allows for the dramatic enhancement of such processes as Raman scattering (Surface Enhanced Raman Scattering - SERS), second harmonic generation, photoluminescence and charge transfer for the molecular and solid nanoobjects in the vicinity of the metal nanostructures [10-18]. The effect of SERS is based on the giant enhancement of the scattering cross-section of the molecules adsorbed on nanostructured metal surface (SERS-substrate) or on free-standing metal

nanoparticles. For the SERS effect to take place, the size of the NPs or surface texture of the substrate should be smaller than the wavelength of exciting laser light. The enhancement of Raman signal in SERS processes can be as much as several order of magnitude and strongly depends on the sort of metal (usually silver or gold), characteristic size of metal nanostructures, their shape and interparticle distance. Up to now, a lot of experimental and theoretical work has been done in the field, aimed at building a general model of the plasmon-mediated enhancement of the optical response of molecules and solids in the vicinity of metal nanostructures [19]. Though such a model is not existing yet even for most intensively studied process of Raman scattering, it is established that the dominant contribution to the SERS-effect is made by the concentration of electric field of the exciting light near the surface of metal nanostructures (electromagnetic mechanism) due to the excitation of surface or/and localized plasmons in them [18]. Additional

enhancement comes from molecule-metal charge transfer, but only in particular cases of molecules chemically bound to the metal [18]. The latter (chemical) mechanism, contrary to more extended electromagnetic enhancement, thus works only for the first layer of deposited molecules. Most of SERS studies are performed on randomly roughened metal surfaces (island films) or random aggregates of metal nanoparticles. The efforts of numerous research groups over the world are directed towards obtaining inexpensive substrates with ordered morphology of the nanostructured metal, which would provide better control over the spectral parameters of plasmon resonance and reproducibility of the enhancement magnitude. The desired technology should therefore allow for both parameters of the individual metal nanoparticles (size, shape) and their placement on the substrate surface (ordering, interparticle distance) to be controllable. One of the main methods of obtaining SERS-substrates today is thermal deposition of nm-thick noble metal films (silver or gold) with their subsequent thermal annealing [3, 7, 18]. The drawback of this method is a low quantitative reproducibility of the SERS enhancement – both between substrates and between different spots over the same substrate.

This work was aimed at development of efficient SERS-substrates with homogeneous enhancement over the whole substrate for both laterally disordered (random) and laterally ordered gold nanostructures, as well as comparison of their plasmonic properties and SERS-enhancement, with the Rhodamine 6G chosen as analyte.

2. Experimental

The SERS substrates based on the laterally disordered ensembles of Au nanoislands were grown by the thermal deposition of Au onto glass substrates in vacuum (10^{-7} Pa). The nominal thickness of the gold deposited was varied between 1 and 12 nm at the step of 1 nm. The film thickness was controlled in-situ by quartz resonator. The as-deposited films were annealed for 10 min in air; the annealing temperature, T_{ann} , was varied from 250 to 450°C at the step of 50°C.

The laterally ordered SERS substrates were formed on two-dimensional holographic grating created in polymer layer on glass substrate. The period of the polymer grating in both (perpendicular) directions was varied from 350 to 500 nm and was determined by the laser wavelength used for writing the hologram (He-Cd- and Ar⁺-lasers). The formed polymer gratings were covered by layer of Au with the nominal thickness varied from 4 up to 50 nm. Au deposition was performed using the same thermal evaporation technique as for laterally disordered films.

Optical transmission and reflection spectra of the SERS substrates under study were measured at Shimadzu UV-3600 spectrometer. Surface morphology was studied with scanning electron microscope (SEM)

Mira 3 Tescan. Raman spectra were excited with different wavelengths of Ar⁺-Kr⁺ laser and registered with Jobin Yvon T64000 spectrometer. Rhodamine 6G (Rh6G) was used as analyte to estimate SERS-properties of the substrates.

3. Results and discussion

SERS substrates with laterally disordered ensembles of Au nanoislands.

At the first stage of this work, we investigated the laterally disordered ensembles of Au nanoislands obtained by thermal deposition of Au on glass slides. It was found that flat Au films thinner than about 10 nm are unstable in air towards transition to nanoislands. The size of the nanoislands, and therefore the spectral position of the plasmon resonance, was found to depend on the nominal film thickness. As far as the self-induced transformation of the flat Au film into the island film is a very slow process at room temperature, with the duration of transformation increasing with increase of the nominal film thickness, the as-deposited films were annealed in order to accelerate formation of nanoislands. Moreover, the annealed films revealed much better stability of their parameters, up to 6 months, as compared with substrates based on self-induced formation of nanoislands.

Another important factor that influences dramatically morphology of the island film is temperature of the thermal annealing. We performed a detailed SEM study of both the 2D-3D transformation and subsequent growth of 3D islands for various nominal Au thicknesses, but shown in Fig. 1 are only representative results for $t_{\text{nom}}=4$ nm. It is seen from the Fig. 1 that both the size and shape of the nanoislands are strongly dependent on T_{ann} . Already at $T_{\text{ann}}=250^\circ\text{C}$, the 4 nm thick Au films transform into labyrinth-shaped island morphology (Fig. 1, b). Further increase of T_{ann} up to 300°C leads to reduction of the islands' length and increase of islands' width (Fig. 1, c-d). After that, in the T_{ann} range 400-450°C, the bimodal island ensembles are formed with spherical and ellipsoidal base shapes (Fig. 1, e-f).

We observed the similar scenario of morphological transformation for films with various t_{nom} . However, the T_{ann} at which 2D-3D transformation occurs increases with t_{nom} .

Variation of annealing duration at given T_{ann} did not lead to noticeable changes in island morphology and optical characteristics of the substrates. Optical absorption study of as-deposited films shows that the maximum of plasmon absorption shifts to longer wavelengths with increase of t_{nom} (Fig. 2, a). This shift can be explained by increase of the average island size.

The annealing of the films leads to noticeable changes in morphology and optical spectra. As seen from Fig. 2, b, the absorption bands shift to shorter wavelength and become much narrower after annealing. A doublet structure observed for 2 and 4 nm films is

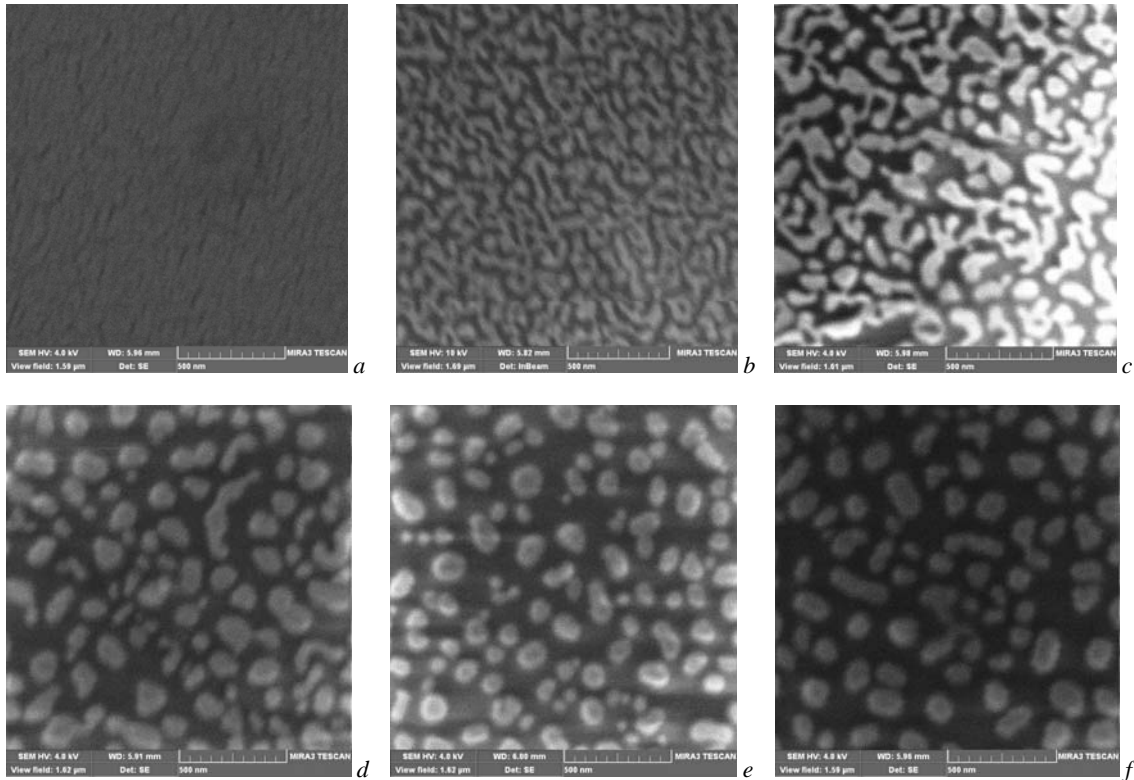


Fig. 1. SEM-images of nanoisland films obtained from as-deposited (a) 4 nm film by annealing at 250 (b), 300 (c), 350 (d), 400 (e) and 450°C (f) for 10 min.

very interesting and should be discussed. Two mechanisms can be considered to explain this doublet in absorption. Firstly, the nanoislands of elongated ellipsoidal shape in these samples may support two plasmon modes, along and perpendicular to the long axis, with different plasmonic frequencies. Secondly, the bimodal distribution of island shapes (with spherical and ellipsoidal bases) can be responsible for two maxima in plasmon absorption spectra.

Though further investigations are in progress to evaluate contribution of each of two mechanisms, the results already obtained show that variation of the nominal thickness of Au films (Fig. 2) and temperature of their annealing within the range 250-450°C (Fig. 3) are efficient tools when tuning the plasmon properties of SERS-substrates.

Moreover, if the nominal film thickness is homogenous over the sample surface, morphology of the annealed film will be also homogenous, and we can obtain the SERS substrate with homogeneous enhancement properties over its whole surface.

In order to further increase the efficiency of the SERS-substrates, the intensity of the plasmon absorption bands is to be increased and their width reduced. This can be achieved by increasing the annealing time. But the drawback of this way is formation of bimodal shape distribution of the islands, as well as different inter-island distances. Another way to better homogeneity (as well as controllable ordering) of the island ensemble is a pre-patterning of the substrate surface.

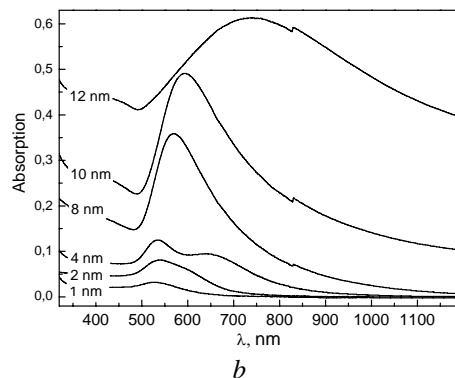
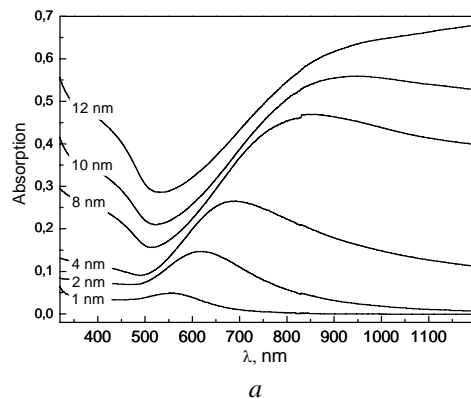


Fig. 2. Optical absorption spectra of the as-deposited (a) and annealed at 400°C (b) Au films of various t_{nom} (indicated).

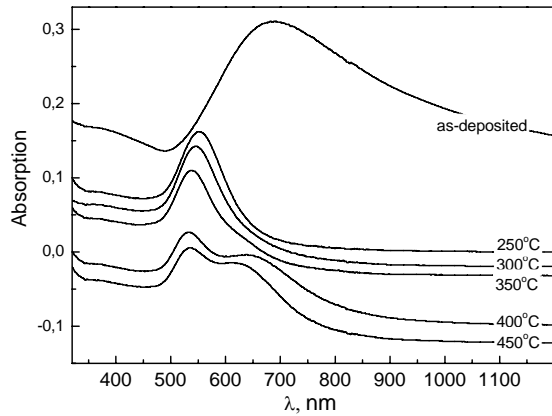


Fig. 3. Optical absorption spectra of the as-deposited and annealed Au films of $t_{\text{nom}}=4$ nm.

SERS substrates with laterally ordered ensembles of Au nanoislands.

In order to obtain the laterally ordered and homogenous ensembles of Au nanoislands, pre-patterning of the substrate was made by a holographic method. Moreover, the Au nanoislands dimensions possible to be achieved by this method, $\sim 100\text{nm}$, were expected to provide the plasmon absorption in the red and infrared regions ($\lambda \geq 700$ nm) [20, 21]. This region is, in particular, the

transparency window for the human tissues and therefore these SERS substrates can be employed for in-vitro Raman studies of drug delivery or diagnostics of diseases within human cell.

The main challenge of our method to obtain the SERS substrates was optimization of the nominal thickness of Au deposited on polymer islands preliminary formed by photolithography. At small t_{nom} , we expected small nanoislands to be formed on polymer surface, at high t_{nom} either the continuous film was expected or a discontinuous morphology with predominant filling of the dips between the polymer islands. The latter two morphologies would obviously have different spectra of plasmon absorption.

Fig. 4 shows SEM-images of the polymer islands covered with different nominal thicknesses of Au. It is seen that morphology of Au film noticeably depends on t_{nom} . We did not observe expected small Au nanoislands at low t_{nom} . Instead, a quasicontinuous film is formed up to $t_{\text{nom}}=5$ nm (Fig. 4, a), and at increase of t_{nom} up to 16 nm a net of cracks is formed (Fig. 4, b, c). Note, the qualitatively similar morphologies we observed for Au of the same t_{nom} deposited onto flat polymer surface. The revealed difference in morphology of Au films formed on polymer (Fig. 4) and glass (Fig. 1) is obviously due to the different energy of the interface Au/glass and Au/polymer [18]. Note that continuous (i.e. without cracks) Au film on polymer can be formed only at

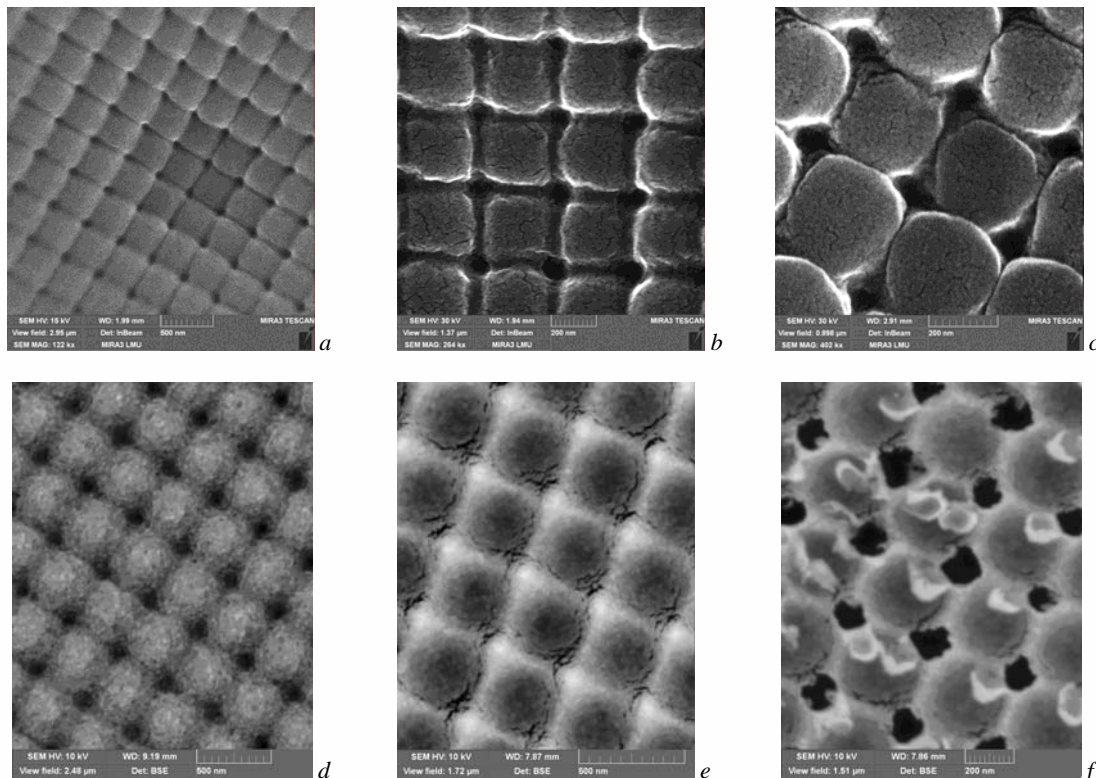


Fig. 4. SEM-images of the polymer islands covered with different nominal thicknesses of Au: 5 (a), 12 (b), 16 (c), 30 (d), 40 (e), and 45 nm (f).

$t_{\text{nom}}=30\text{-}35\text{ nm}$ (Fig. 4, d). Further increase of t_{nom} leads to formation of cracks again, but in this case they are larger and concentrated in the areas between the islands (Fig. 4, e). After cutting the sample into smaller pieces, we observed formation of highly homogeneous holes, exactly at the places of maximum concentration of cracks – where corners of four neighboring islands meet (Fig. 4, f). Formation ("opening") of the holes we relate with relaxation of the mechanical stress accumulated in the Au film between the islands. The critical t_{nom} at which the stress is relieved via formation of holes is about 45 nm (Fig. 4, f).

In order to choose the optimum excitation wavelength for SERS-investigations of the Rh6G molecules adsorbed on the surface of laterally ordered Au nanostructures, their optical absorption spectra were studied (Fig. 5).

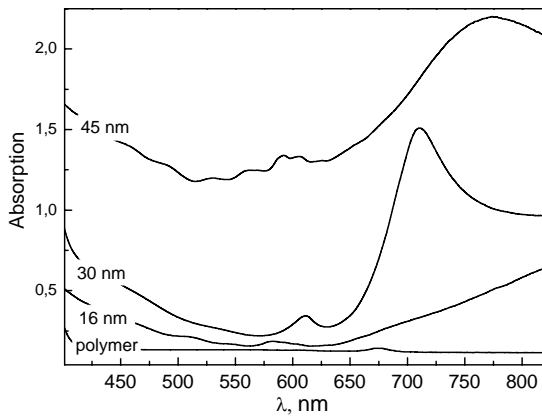


Fig. 5. Optical absorption spectra of polymer substrate before and after deposition of Au film with t_{nom} equal to 16, 30 and 45 nm.

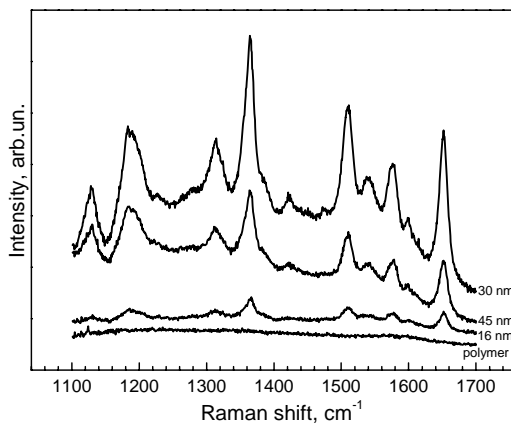


Fig. 6. Raman spectra of Rh6G deposited onto a bare polymer substrate and nanostructured Au films with t_{nom} equal to 16, 30 and 45 nm.

Analysis of the optical absorption spectra for the substrates after deposition of the relatively thick nominal thickness of Rh6G molecules was found to lead to the red shift of the plasmon maximum (not shown). In the case of deposition of low-concentration Rh6G solution, used in the present study for evaluation of the enhancement properties of the SERS substrates, the effect of the adsorbed molecules on optical properties of Au nanostructure was negligible.

As can be seen from the Fig. 5, the plasmon resonance of the island film with 45 nm nominal Au thickness fits well the transparency window of living tissues 750-1050 nm [22], and therefore this kind of SERS substrates can find applications in biodiagnostics. The presence of holes between the islands can activate the effect of the so-called "hot spots", that is the spots of maximum concentration of plasmon field between the island corners. Driven by the capillary forces, the analyte solution will fill the hole, and the enhancement of Raman signal from the analyte molecules in these spots will be especially strong.

As to the absorption spectrum of the films with $t_{\text{nom}}=30\text{ nm}$, its plasmon maximum, at 710 nm, also fits the above mentioned transparency window. Besides, this sample possesses a rather small width of the plasmon resonance – less than 60 nm.

The maximum enhancement of Raman signal of the analyte molecules deposited onto the SERS substrate is known to be achieved at the excitation wavelength, λ_{exc} , being within the spectral range of the plasmon band. The lasers commonly available for Raman measurements have a discrete set of wavelengths, which do not cover the whole spectral range of plasmon resonances of noble metals. For this reason, the adjustment of the structural and morphological parameters of the SERS substrate is necessary to tune its plasmon absorption in resonance with available λ_{exc} .

Fig. 6 shows the Raman spectra of Rh6G obtained with $\lambda_{\text{exc}}=676.4\text{ nm}$. For these measurements, we used the solution with Rh6G concentration 10^3 lower than that at which Raman signal could be registered without enhancement. As expected, no Raman signal was registered at this concentration on bare polymer island film (Fig. 6, bottom curve). The same concentration of analyte on substrates with various t_{nom} of Au gives high Raman signals (Fig. 6, upper curves). In this case, the highest signal was obtained for $t_{\text{nom}}=30\text{ nm}$, with the enhancement factor being as high as 10^4 . When using λ_{exc} more close to the plasmon maximum, for example, 695- or 705-nm lasers for 30 nm thick Au film or 785-nm laser for the 45-nm film, even much higher enhancement factors can be achieved with these SERS substrates.

An additional enhancement of the Raman signal is caused by the mentioned above "hot spots" between the islands [19]. This effect is actual only for the molecules adsorbed in the area between the islands. As far as in our Raman experiments the laser spot was $\sim 1\mu\text{m}$, the

obtained enhancement factor of 10^4 is an average of contribution from the molecules situated both in the "hot spots" and on the surface of islands. Thus, the local enhancement in the "hot spots" can be much higher. The evaluation of this local enhancement is one of the tasks for the future work.

4. Conclusion

Technology of SERS substrates have been developed for efficient and laterally homogenous enhancement of the Raman signal from molecular analytes. Laterally ordered and disordered arrays of Au nanoislands are found to be capable of efficient SERS effect. The dependence of the SERS-effect on the morphology of substrates was studied. The parameters of the islands' morphology and their plasmon resonance depend noticeably on the nominal Au thickness and annealing temperatures. The mechanism of Au islands formation on polymer surfaces is found to differ dramatically from that of Au on glass. Formation of nanoholes in the case of Au substrates on holographically pre-patterned polymer film opens up the possibility of additional enhancement via the "hot spot"-effect. Technology developed by us allows to obtain SERS substrates exhibiting plasmon resonance within the spectral range 700-900 nm that falls into the transparency window of human tissues. These substrates are thus suitable for Raman diagnostics diseases and monitoring drug delivery.

Acknowledgements

The work was supported by NAS of Ukraine (project № 3.5.3.4/6-DP), Fund for Fundamental Research of Ukraine (F40.2/068, F40.1/017), Russian Foundation for Basic Research (11-02-90427-Ukr-f-a) and Alexander von Humboldt Foundation.

References

1. K.L. Kelly, E. Coronado, L.L. Zhao, G.C. Schatz, The Optical Properties of Metal Nanoparticles: The Influence of Size, Shape, and Dielectric Environment // *J. Phys. Chem. B* **107**, p. 668-677 (2003).
2. P.N. Bartlett, J.J. Baumberg, S. Coyle, M. E. Abdelsalam, Optical properties of nanostructured metal films // *Faraday Discuss.* **125**, p. 117-123 (2004).
3. G. Xu, M. Tazawa, P. Jin, S. Nakao, Surface plasmon resonance of sputtered Ag films: substrate and mass thickness dependence // *Appl. Phys. A* **80**, p. 1535-1540 (2005).
4. M.B. Cortie and A. M. McDonagh, Synthesis and Optical Properties of Hybrid and Alloy Plasmonic Nanoparticles // *Chem. Rev.* **111**, p. 3713-3735 (2011).
5. A.M. Kelley, A molecular spectroscopic view of surface plasmon enhanced resonance Raman scattering // *J. Chem. Phys.* **128**, p. 224702 (2008).
6. W.L. Barnes, Comparing experiment and theory in plasmonics // *J. Opt. A: Pure Appl. Opt.* **11** p. 114002 (2009).
7. N.L. Dmitruk, A.V. Korovin, O.I. Mayeva, M.V. Sosnova, Role of Local Plasmons in Interaction of Light with 1D Periodic Ensembles of Metallic Nanowires // *Plasmonics* **4**, p. 193-200 (2009).
8. M. Lončarić, J. Sancho-Parramon, H. Zorc, Optical properties of gold island films - a spectroscopic ellipsometry study // *Thin Solid Films* **519**, p. 2946-2950 (2011).
9. P. Cheyssac, V.A. Sterligov, S.I. Lysenko, R. Kofman, Surface Plasmon-Polaritons // *Phys. Stat. Sol. (a)* **175**, p. 253-258 (1999).
10. E.V. Klyachkovskaya, N.D. Strelak, I.G. Motevich, S.V. Vashchenko, M.Ya. Valakh, A.N. Gorbacheva, M.V. Belkov, S.V. Gaponenko, Enhancement of Raman Scattering by Ultramarine Using Silver Films on Surface of Germanium Quantum Dots on Silicon // *Optics and Spectroscopy* **110**, p. 48-54 (2011).
11. S. Roh, T. Chung, B. Lee, Overview of the Characteristics of Micro- and Nano-Structured Surface Plasmon Resonance Sensors // *Sensors* **11**, p. 1565-1588 (2011).
12. K. Hering, D. Cialla, K. Ackermann, T. Dorfer, R. Moller, H. Schneidewind, R. Mattheis, W. Fritzsche, P. Rosch, J. Popp, SERS: a versatile tool in chemical and biochemical diagnostics // *Anal Bioanal Chem* **390**, p.113-124 (2008).
13. S. C. Warren and E. Thimsen, Plasmonic solar water splitting // *Energy Environ. Sci.* **5**, p. 5133 (2012).
14. C.-C. Chang, Y. D. Sharma, Y.-S. Kim, J. A. Bur, R. V. Shenoi, S. Krishna, D. Huang, S.-Y. Lin, A Surface Plasmon Enhanced Infrared Photodetector Based on InAs Quantum Dots // *Nano Lett.* **10**, p. 1704-1709 (2010).
15. S. N. Terekhov, P. Mojzes, S. M. Kachan, N. I. Mukhurov, S. P. Zhvavyi, A. Yu. Panarin, I. A. Khodasevich, V. A. Orlovich, A. Thorel, F. Grillond and P.-Y. Turpine, A comparative study of surface-enhanced Raman scattering from silver-coated anodic aluminum oxide and porous silicon // *J. Raman Spectrosc.* **42**, p. 12-20 (2011).
16. R. Alvarez-Puebla, B. Cui, J.-P. Bravo-Vasquez, T. Veres, H. Fenniri, Nanoimprinted SERS-Active Substrates with Tunable Surface Plasmon Resonances // *J. Phys. Chem. C* **111**, p. 6720-6723 (2007).
17. M.V. Chursanova, L.P. Germash, V.O. Yukhymchuk, V.M. Dzhagan, I.A. Khodasevich, D. Cojoc, Optimization of porous silicon preparation technology for SERS applications // *Appl. Surf. Sci.* **256**, p. 3369-3373 (2009).

18. M.V. Chursanova, V.M. Dzhagan, V.O. Yukhymchuk, O. S. Lytvyn, M.Ya. Valakh, I.A. Khodasevich, D. Lehmann, D.R.T. Zahn, C. Waurisch, S.G. Hickey, Nanostructured silver substrates with stable and universal SERS properties: application to organic molecules and semiconductor nanoparticles // *Nanoscale Res Lett* **5**, p. 403-409 (2010).
19. K. Kneipp, M. Moskovits, H. Kneipp (eds.), *Surface-Enhanced Raman Scattering: Physics and Applications*, Springer, Berlin, 2006.
20. J.D. Driskell, R.J. Lipert, M.D. Porter, Labeled gold nanoparticles immobilized at smooth metallic substrates: systematic investigation of surface Plasmon resonance and surface-enhanced Raman scattering // *J. Phys. Chem. B* **110**, p. 17444-17451 (2006).
21. N.Felidj, J.Aurbard, G. Levi, J.R. Krenn, M. Salerno, G. Schider, B. Lamprecht, A. Leitner, F.R. Aussenegg, Controlling the optical response of regular arrays of gold particles for surface-enhanced Raman scattering // *Phys. Rev. B*, **65**, p. 075419 (2002).
22. V.V. Tuchin (Ed.) *Handbook of Optical Biomedical Diagnostics*. SPIE Press, Washington, 2002.